NASA CONTRACTOR REPORT

NASA CR-533

NASA CR-533

A THERMISTOR ARRANGEMENT TO IMPROVE TEMPERATURE MEASUREMENTS AT HIGH ALTITUDES

by William A. Drews

Prepared by
ATLANTIC RESEARCH CORPORATION
Alexandria, Va.
for Langley Research Center

NATIONAL AERONAUTICS AND SPACE ADMINISTRATION • WASHINGTON, D. C. • AUGUST 1966

NASA CR-533

A THERMISTOR ARRANGEMENT TO IMPROVE TEMPERATURE MEASUREMENTS AT HIGH ALTITUDES

By William A. Drews

Prepared under Contract No. NAS 1-1611 by
ATLANTIC RESEARCH CORPORATION
Alexandria, Va.

for Langley Research Center

NATIONAL AERONAUTICS AND SPACE ADMINISTRATION

For sale by the Clearinghouse for Federal Scientific and Technical Information
Springfield, Virginia 22151 – Price $2.00

ABSTRACT

A design configuration has been developed for supporting the 0.010 inch diameter bead thermistor. This sensor is routinely employed as an immersion thermometer to measure the air temperature over the approximate altitude interval 30 to 65 kilometers. Theory indicates that devices having physical properties similar to those of the bead thermistor can be used to obtain accurate temperature data up to the region of 65 kilometers. The development described attempts to achieve thermal isolation of the thermistor so that theoretical capability can be realized in practice.

The design is analyzed from the standpoint of its thermal model, the input of a standard atmospheric profile and, the dynamic thermal conditions imposed by a parachute lowered instrument. Results of the analysis show that the described system should yield ambient temperature values within 2% below 54 km and within 5% at 60 km. Above 60 km the accuracy deteriorates rapidly with altitude increase. Lowering of initial equilibrium temperature of the thermistor does not materially improve accuracy; neither does increasing the initial altitude of exposure of the sensor. The most marked improvement results from lowering the ventilation speed.

ACKNOWLEDGEMENT

The author wishes to express his gratitude to others on the technical staff of Atlantic Research Corporation who have contributed to the development of the device described herein and to the theoretical analysis of its performance. In particular appreciation is expressed to Mr. L. H. Washington for development effort and to Messrs. D. Fisher and D. Holter whom assisted, respectively, in the theoretical analysis and the computer programming.

TABLE OF CONTENTS

LIST OF ILLUSTRATIONS

I. INTRODUCTION

A quantitative description of the earth's atmosphere, to very high altitude, is of intense interest to modern science. Among specific regions of interest is that in which the atmosphere is known to behave in the manner of an ideal gas i.e.; the region in which constituents are well known and the equation of state of an ideal gas may be applied. Thus parameters of temperature, pressures, and density of the gas at any designated altitude up to 260,000 feet are desired.

Until about 1959 the expense of measuring systems for such data acquisition above about 100,000 feet prohibited synoptic data collection programs. Prior to this only wind data, as obtained from the ground based track of chaff dispensed by Loki-Dart rockets, could be afforded on a frequent basis. The development and introduction of the ARCAS meteorological rocket to the meteorological community about 1959 provided a new opportunity to the interested scientist for in situ measurements of such parameters as temperature, pressure, and density, in addition to retaining the wind measuring capability of earlier systems. This rocket system provided sufficient performance, in terms of allowable payload weight and volume, to enable telemetering instruments and on board sensors to be carried to an altitude of approximately 200,000 feet from a sea level launch.

During 1959 the U.S. Army Signal Corps undertook the development of instrumented payloads for the ARCAS rocket. These had as a prime function the measurement and telemetering of atmospheric temperature data from apogee altitude of the rocket downward to at least the region of 70,000 feet where data could be compared with that obtained by balloon-borne radiosondes.

The earlier development of tiny bead thermistors, which were thought to offer promise as an immersion thermometer for temperature measurement at such altitudes, formed a basis of design concept for these instruments, from the sensor standpoint. A number of investigators have undertaken study and analysis of the small (0.010 inch diameter) bead thermistor as an immersion resistance-type thermometer for use at very high altitude. In general, the results of these studies indicated that temperatures could be measured within reasonable accuracy (1 - 2%) to altitudes in the order of 200,000 feet. In practice, however, reduced data from many soundings have shown that temperature data of reasonable values was not being consistently obtained at altitude much above about 150,000 feet. A review of theoretical analyses and comparison of actual sensor performance led the contractor to conclude that the problem rested with inadequacy in the design of the method of mounting the thermistor. It was felt that a rigorous treatment of all potential error sources in design could result in a mounting method which would enable realization of the theoretical altitude capability of the thermistor as an immersion thermometer.

The National Aeronautics and Space Administration's Langley Research Center sponsored a development program, under Contract NAS1-1611, aimed at improving the altitude to which temperature data could be accurately obtained with these bead thermistors. It is the results of this effort which is herein reported.

II. THEORETICAL CONSIDERATIONS

A - Basic Concepts

Of concern here is the measurement of the temperature of a gas, the atmosphere, by means of immersion thermometry. Ideally the air thermometer used for such purposes should always be in thermal equilibrium with the gas; should be at very nearly the same temperature as the gas and; should maintain the foregoing relations despite any changes in the gas temperature. To evaluate the capability of a thermometer for this purpose it is necessary to analyze, for small temperature differences, the relative magnitudes of the power loss by radiation and the power loss by convection and conduction because the thermometer is thermally coupled to the gas by its conduction, or convection.

Ney [1], e.a., have analyzed air thermometers of the resistance type by examining the behavior of fine wires and small thermistors. From the analysis several important conclusions may be drawn as follows:

> To reduce radiative effects on a thermometer, it is necessary to reduce its size as much as is practical and to provide a surface which is highly reflective to long wave radiation.
>
> At those pressures wherein the dimension of the thermometer is larger than a mean free molecular path, the conduction is essentially independent of the gas pressure, and the heat transfer per unit dimension per unit of temperature difference is essentially constant. Contrarily, at pressures wherein the mean free molecular path is comparable to and larger than the dimension of the thermometer, the conduction becomes a strong function of the gas pressure.

Forced ventilation does not contribute to the power loss from an air thermometer when the gas pressure is below about 2 millibars.

From the above it may be seen that a tradeoff can be made between the desired reduction in size of the thermometer for radiative purposes and the desired maintenance of size from the standpoint of its dimension versus the mean free path of the gas. Stated differently: while radiative effects are important, the size also places a limitation on the altitude to which a given thermometer can be used to measure air temperature. Since the mean free molecular path at 60 kilometers altitude is approximately 0.0126 inches (12.6 mils), it follows that this altitude is nearly the maximum to which the 10 mil bead thermistor can be used as an air thermometer.

B - Thermal Analysis

To determine an estimate of the probable accuracy of an air thermometer, it is necessary to develop the energy balance equation for the device under all conditions to which it will be subjected. Hence for the case of the small bead thermistor, used in high altitude sounding rockets, both static and dynamic heat input and heat loss parameters must be examined along with the thermal properties of the thermistor.

Barr[2], Wagner[3], Ballard[4], and Wright[5] have assessed the probable performance of the bead thermistor for sounding rocket use when the sensor is lowered through the atmosphere by parachute. In Barr's analysis the sensor is treated as a free body, unattached to any mounting. Hence, except for assumptions made with regard to fall velocity and assuming that the constants used are valid, a fair prediction of the theoretical accuracy of the bead is obtained therefrom. Of special interest therein are the values of measuring error which are attributed to radiative effects. These range from approximately 0.6 degree K at 58 kilometers to 0.1 degree at 30 kilometers.

Wagner carried a similar analysis farther by including heat transfer parameters which are associated with the fact that resistance sensors must always be attached to some mounting in order to measure their resistance. Hence the error analysis derived from this study more nearly approximates the practical situation. Of interest here is a comparison of the steady state computed error of Barr, which is 2.086°K at 58 km, and the computed error of Wagner, which is 13.5°K at 58 km. Much of this difference may be attributed to the difference in fall velocity used by the two investigators, but some is due to the presence of the thermistor mounting.

C - Problems of Error Reduction

To improve the accuracy obtainable from the 10 mil bead thermistor, it is necessary to examine the various sources of error and their relative contribution to the total. In this way appropriate design approaches can be developed. Little can be done, for example, to reduce radiative error of the aluminum coated thermistor because the properties which control this input are characteristic of the element and the steady state environment to which it is subjected. Moreover, computations indicate that this error is relatively small over the altitude range of interest (30 - 60 Km).

In the same manner, the time constant of the thermistor is a function of its physical properties and the environment to which it is exposed. Hence, without redesign of the sensor, no improvement can be made in its time constant or the system error imposed by this parameter.

Areas for improvement in measuring accuracy must then stem from achievement of thermal isolation between the sensor itself and its mounting and measuring circuits.

III THERMISTOR MOUNT DEVELOPMENT

A - Design Goals

Pursuing the goal of providing a design for mounting of the small bead thermistor which would minimize or eliminate major sources of error, in temperature measurement, the contractor selected several influencing parameters as problem areas for design consideration. These were: thermal isolation of the bead from heating via conducting paths through physical connections; minimization of thermistor lead length to reduce absorption of incident radiation, and; minimization of absorption of electromagnetic energy from the nearby telemetry transmitter.

B - Design Approach

Because of the fragile nature of the bead and its leads, it was felt that mere extension of lead length, as a means of achieving thermal isolation, would be unsuitable. Moreover, it was known that the leads are highly absorptive to solar radiation and, further, that long leads became an effective antenna at the telemetering frequency thus causing absorption of electromagnetic energy by the bead. To circumvent these problem areas the design shown in Figure 1 was first selected.

In this arrangement it was intended that the Mylar film, in conjunction with the thin deposited layer of aluminum, would provide the required degree of isolation of the thermistor from large sources of heat such as the instrument package. Additionally, the Mylar would be relatively transparent to incident solar energy and the aluminum leads, which form the measuring circuit, would be reflective. Thus thermistor leads, which are solar absorptive would be kept very short, about 1/8 inch. The two deposited aluminum strips, in conjunction with a variable capacitor, would also form a radiofrequency transmission line, 1/4 wavelength, at the telemetering frequency. This arrangement would provide an

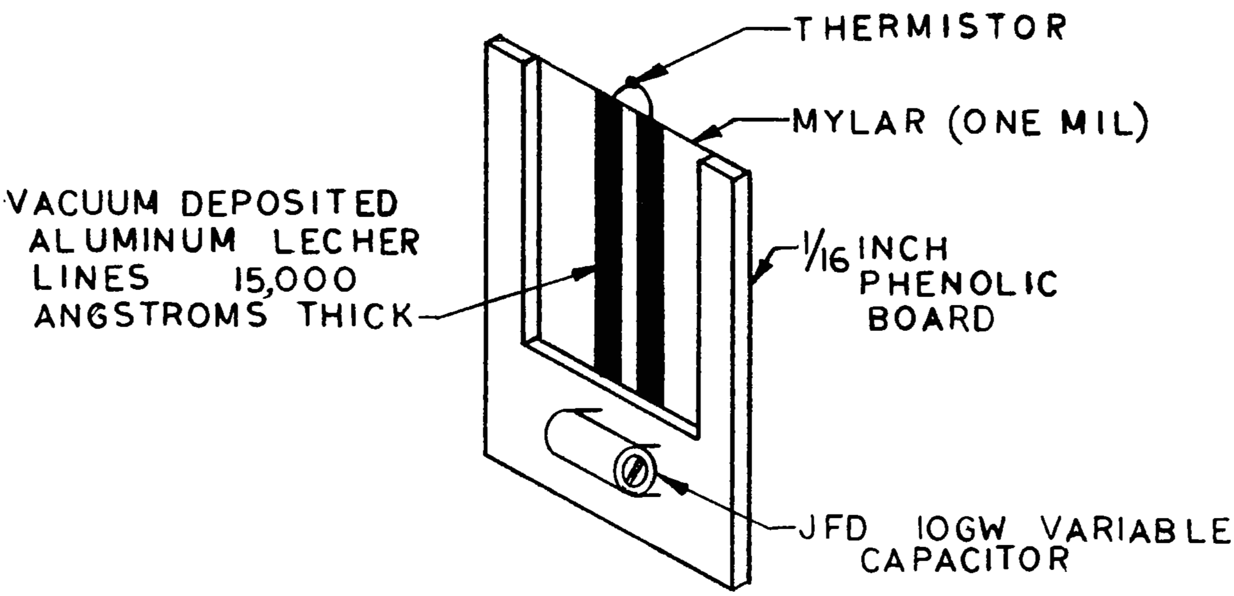

THERMISTOR MOUNTING ASSEMBLY

FIGURE 1

effective short circuit across the thermistor for RF energy while still allowing connections to the aluminum leads for the purpose of measuring the thermistor resistances.

This early model was laboratory tested and found to be effective in preventing the absorption of RF energy. Following this a flight test model was constructed and was installed in an Arcasonde* instrument alongside a mount which had previously been used for temperature data acquisition in these instruments. The commutator of this instrument was arranged so that the two sensors would be alternately sampled, along with the common reference resistor. A flight test was made on September 26, 1962 at NASA, Wallops Island. The results, by comparison, showed considerable improvement in the data which was obtained by the new mount. Table 1 and Figure 2 presents the tabular comparison of the two sensors from this flight. While the graph of Figure 2 depicts data to only 30 kilometers, reference to Table 1 shows that the two thermistors read within one degree of each other as the instrument descended to 15 kilometers.

Following this early flight, with its encouraging data results, design study was undertaken to improve performance, to simplify manufacture, and to reduce costs. Two significant problems faced the contractor: the first being difficulty encountered during assembly of the thermistor leads to the aluminum film; the second being the high cost of the piston type capacitor being used to resonate the transmission line.

Attachment of the thermistor lead to the aluminum film was attempted by the use of a silver epoxy cement. This effort, while successfully flown on a number of tests, provided poor reliability for two reasons; first, because of difficulty in achieving a good bond to the aluminum film, and; second, because even when physical bonds were strong the electrical resistance of the connection

*Tradename of Atlantic Research Corporation.

TABLE 1

DATA FROM TMQ-5 RECORD
WALLOPS ISLAND 9-26-62

Altitude Kilometers	Experimental Mount Temp. - Deg. K	Regular Mount Temp. - Deg. K
52.7	310.1	308.1
52.7	271.1	-
51.9	268.5	301.1
50.9	267.1	298.1
50.3	264.1	293.1
48.8	270.1	291.6
48.0	265.9	290.3
47.5	266.3	286.5
47.0	262.6	286.6
46.3	262.4	286.5
45.7	267.2	285.1
44.9	265.1	283.6
44.2	258.6	282.9
43.6	257.7	276.4
43.3	260.5	-
42.9	259.5	274.1
42.5	256.6	276.1
41.9	251.7	285.1
41.7	255.5	274.1
41.7	-	273.6
40.9	250.4	278.3
40.5	246.1	266.3
40.2	247.1	268.3
39.3	243.6	264.5
39.0	245.6	258.0
38.4	243.6	256.4
37.8	244.1	253.0
37.5	242.8	258.8
37.2	244.1	255.7
36.6	242.8	255.1

Altitude Kilometers	Experimental Mount Temp. - Deg. K	Regular Mount Temp. - Deg. K
36.0	241.3	251.8
35.4	239.8	251.1
34.7	231.8	241.6
33.5	231.1	240.1
32.8	233.1	241.1
32.2	230.5	238.1
31.7	229.3	238.1
31.1	229.7	238.1
30.5	231.3	238.6
27.4	221.3	229.2
24.4	219.1	222.5
21.3	216	220.3
18.3	212	217.1
15.2	209	208.1

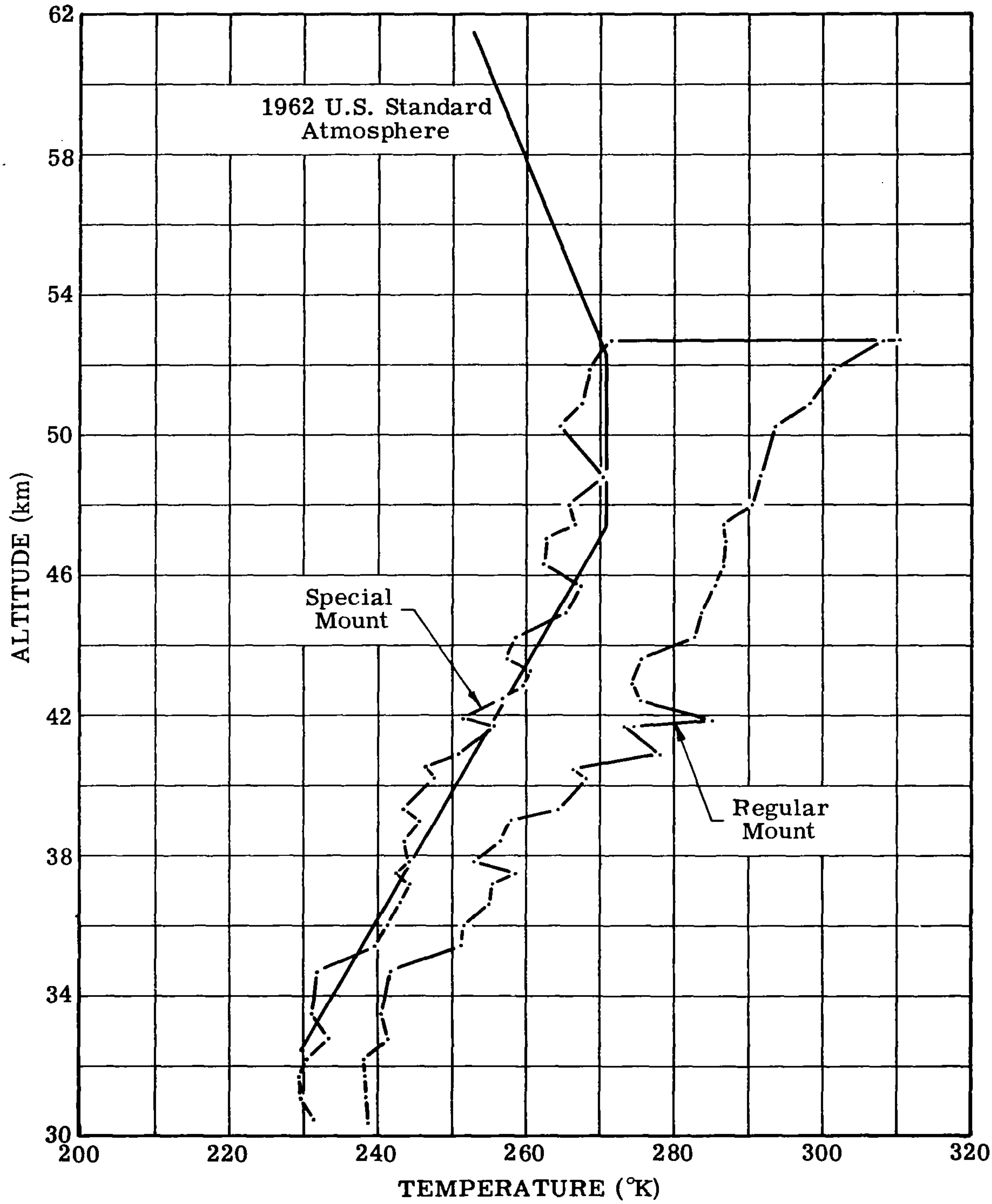

Figure 2. Wallops Island Missile Range, 9-26-62, ARCASONDE IA.

was in the order of 100-200 ohms and was unstable. A number of different silver-epoxy mixes were tried, with little improvement, before a different solution was sought. The final design, which has proven successful employs vacuum evaporation of silver onto the Mylar film, in place of aluminum, and attachment of the thermistor leads to the silver by means of .015 inch diameter solder spheres (see footnote). Drawing EM 40681 depicts the details of this design.

The need for a capacitor to resonate the transmission line was then eliminated by employing strip-line technique to the development of a distributed-constant resonant line. This was accomplished by evaporating two U-shaped silver strips onto opposite faces of the Mylar film in such a way that one leg of each U was exactly opposite that of the other. The lower ends (see drawing) of these center legs are an open electrical circuit while the thermistor leads are attached to the top two ends. A direct current path to the instrument package is provided by the two outer legs. Repeated tests of the effectiveness of this arrangement in preventing RF heating of the bead show that only about 10 microwatts of RF energy is absorbed by the thermistor.

Footnote: Obtained from Circon Components Corporation, Goleta, California.

IV. RESULTS OF FLIGHT TESTS

Since the development of the mount, it has been adopted as standard for the Arcasonde instrument and has been flown routinely at various rocket launch sites which participate in the Meteorological Rocket Network. A few of the temperature-altitude profiles which have been thus obtained are shown in figures 3 through 5. Figure 6 represents a statistical summary compiled by the U. S. Air Force Eastern Test Range of Arcasonde data.

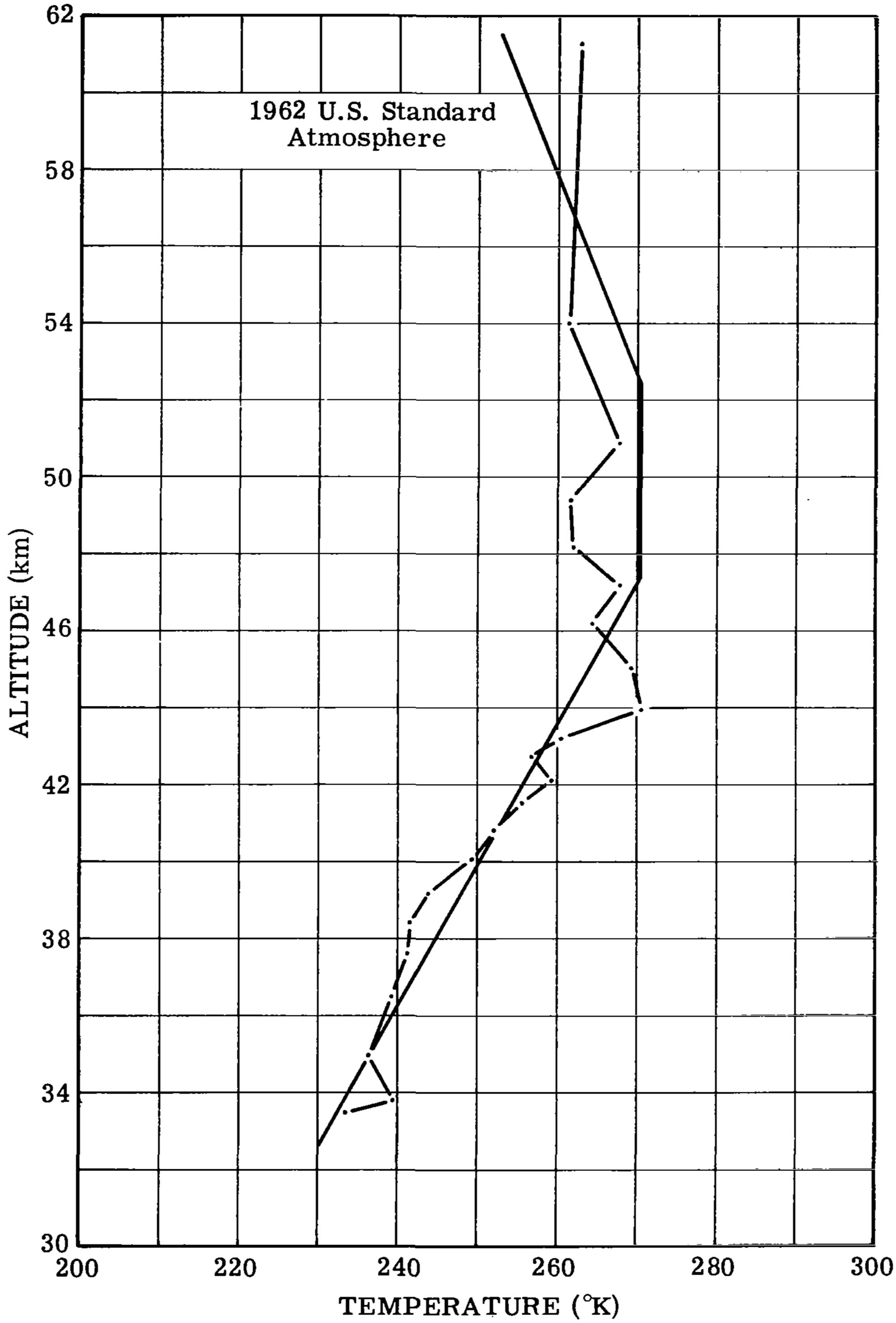

Figure 3. White Sands Missile Range, 1515 GMT 11-24-64, ARCASONDE IA.

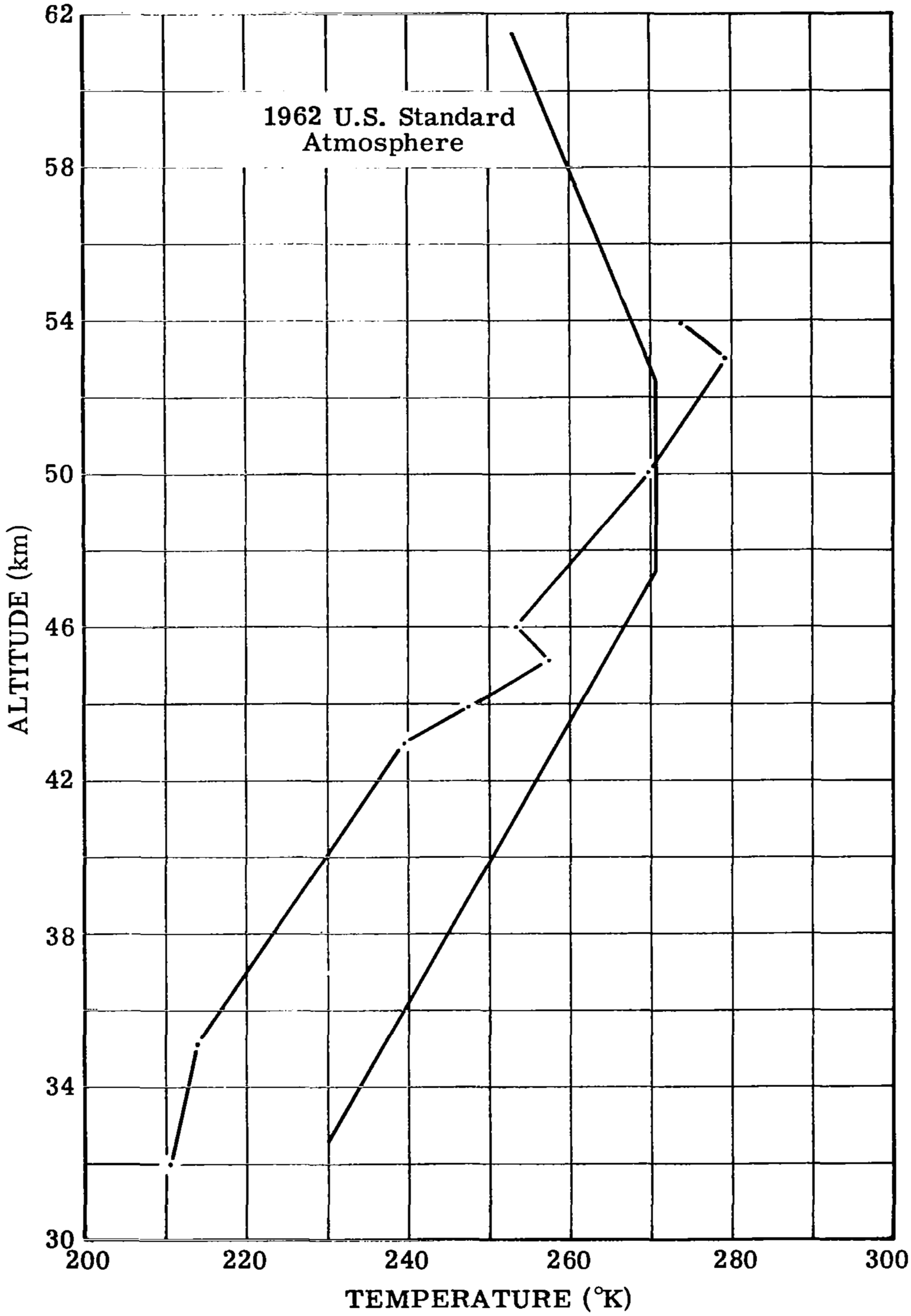

Figure 4. Fort Churchill Missile Range, 0122 Z
1-29-64, ARCASONDE IA.

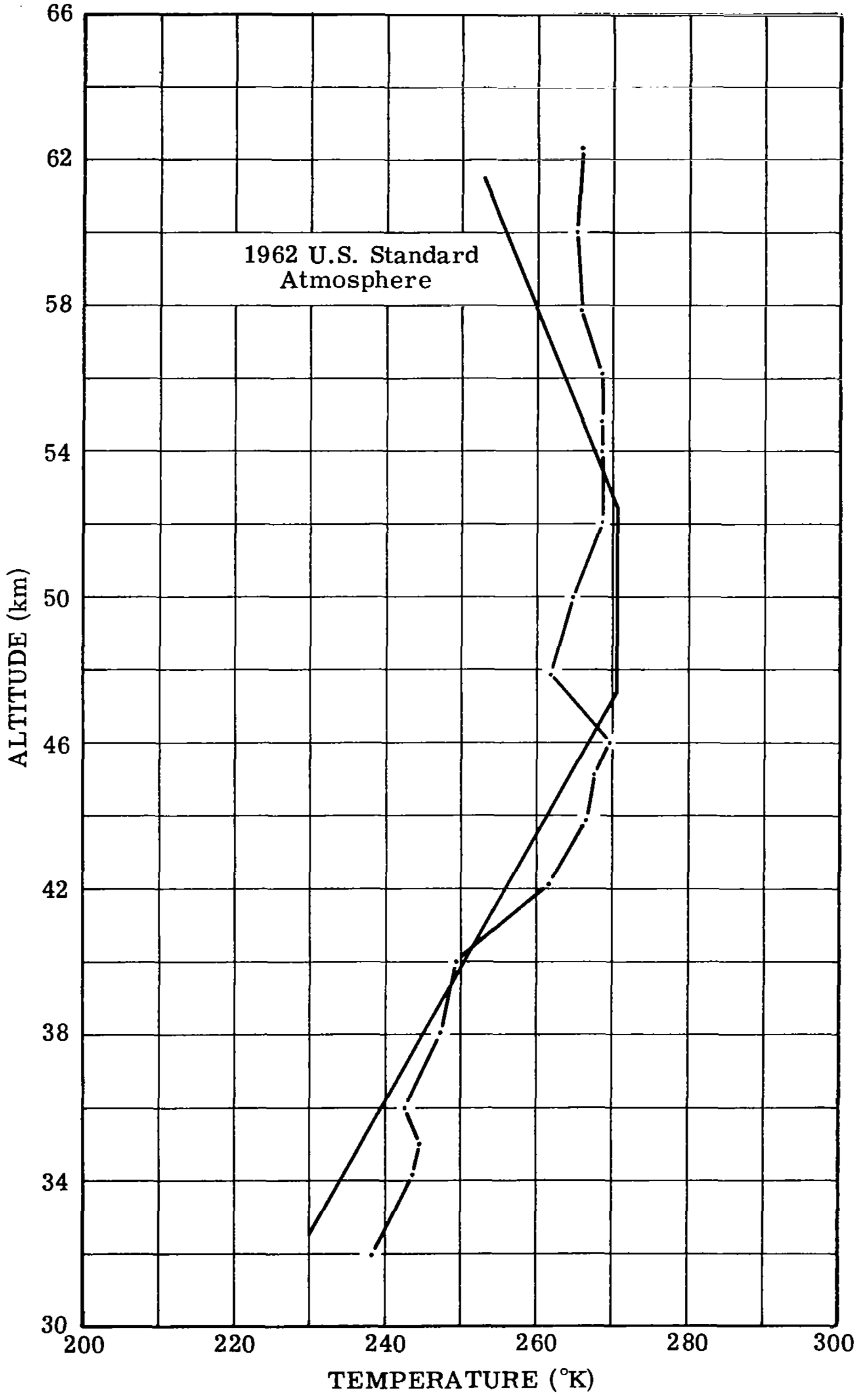

Figure 5. Cape Kennedy Missile Range, 1330 Z 1-25-64, ARCASONDE IA.

FIGURE 6

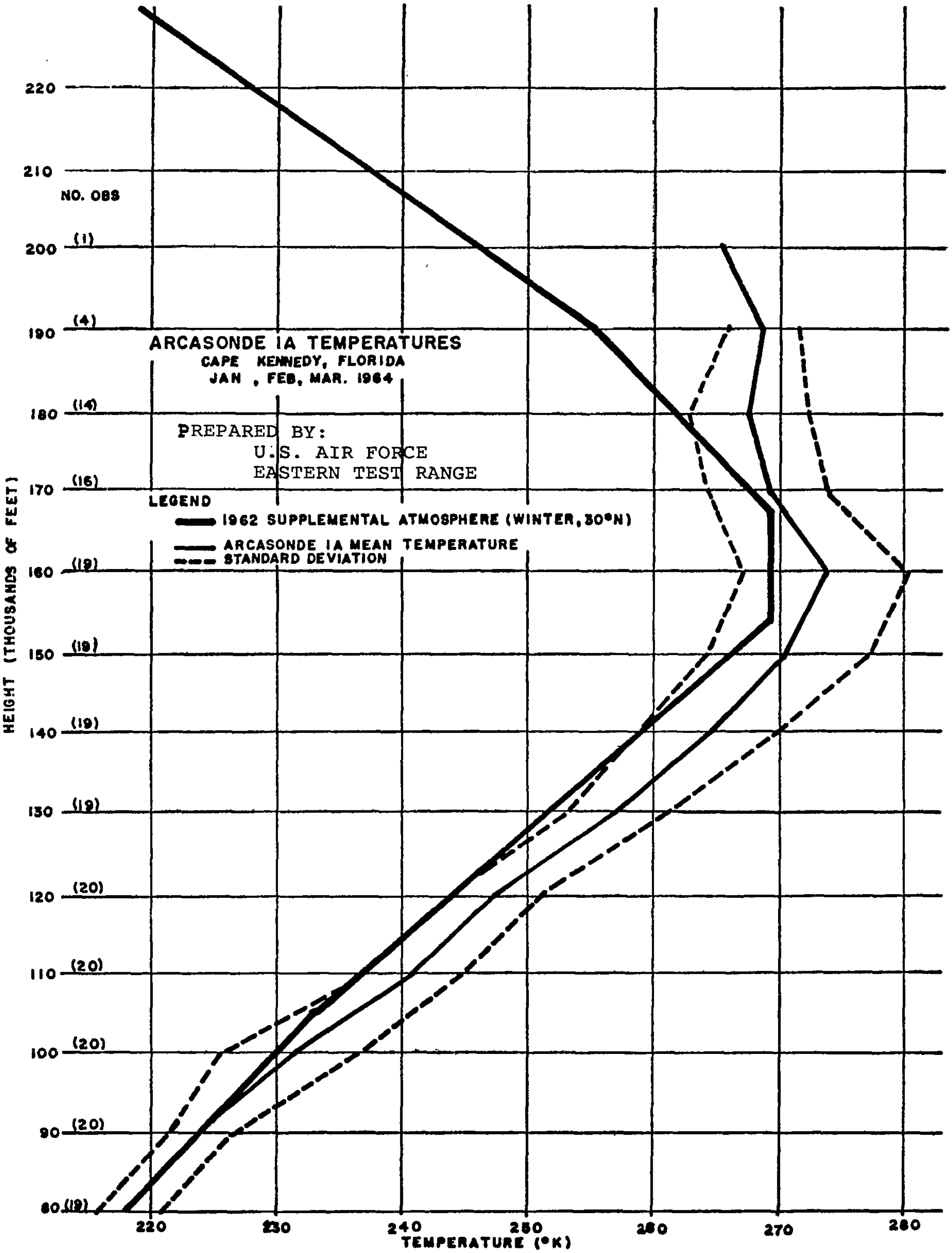

ARCASONDE IA TEMPERATURES
CAPE KENNEDY, FLORIDA
JAN , FEB, MAR. 1964
PREPARED BY:
U.S. AIR FORCE
EASTERN TEST RANGE
LEGEND
1962 SUPPLEMENTAL ATMOSPHERE (WINTER, 30°N)
ARCASONDE IA MEAN TEMPERATURE
STANDARD DEVIATION
NO. OBS
(1)
(4)
(14)
(16)
(19)
(19)
(19)
(19)
(20)
(20)
(20)
(20)
(19)
220
210
200
190
180
170
160
150
140
130
120
110
100
90
80
HEIGHT (THOUSANDS OF FEET)
220
230
240
250
260
270
280
TEMPERATURE (°K)

V. ERROR ANALYSIS

There is no existing standard to which the thermistor and it's mount could be compared during actual high altitude soundings. Moreover the dynamic environment to which the thermistor is normally exposed cannot be readily simulated in a laboratory. Hence, only theoretical analysis remains as an economical tool for assessing the validity of temperature data which is obtained during high altitude soundings.

It was to this problem that Wagner's [3] analysis was addressed, but for a different type of mounting arrangement. The contractor has conducted a similar analysis for the accuracy of the 0.010 inch diameter aluminum-coated bead thermistor when installed on the mount described herein.

A - Basis of Analysis

The thermal model employed in the error analysis is shown in Figure 7. The equations used in solution of this model under the dynamic conditions of a parachute descent as well as a narrative summary of the approach used is given in the Appendix. Other important functions used in the analysis have been adopted from Wagner's [3] study and are repeated in the Appendix for clarity, along with the various constants used in solution of the equations.

Computations have been based upon an initial altitude of 70 kilometers for exposure of the thermistor and an initial velocity of approximately 750 feet per second. While it is recognized that the "fall" velocity is initially zero, the assumption is valid because of the horizontal velocity of the rocket vehicle at the time of expulsion of the instrument. A further assumption made in the computation is that the thermistor, its mount, and the instrument package are all initially in thermal equilibium at $40^{o}C$ (313^{o} Kelvin) and; that the instrument package stays constant at this temperature throughout descent.

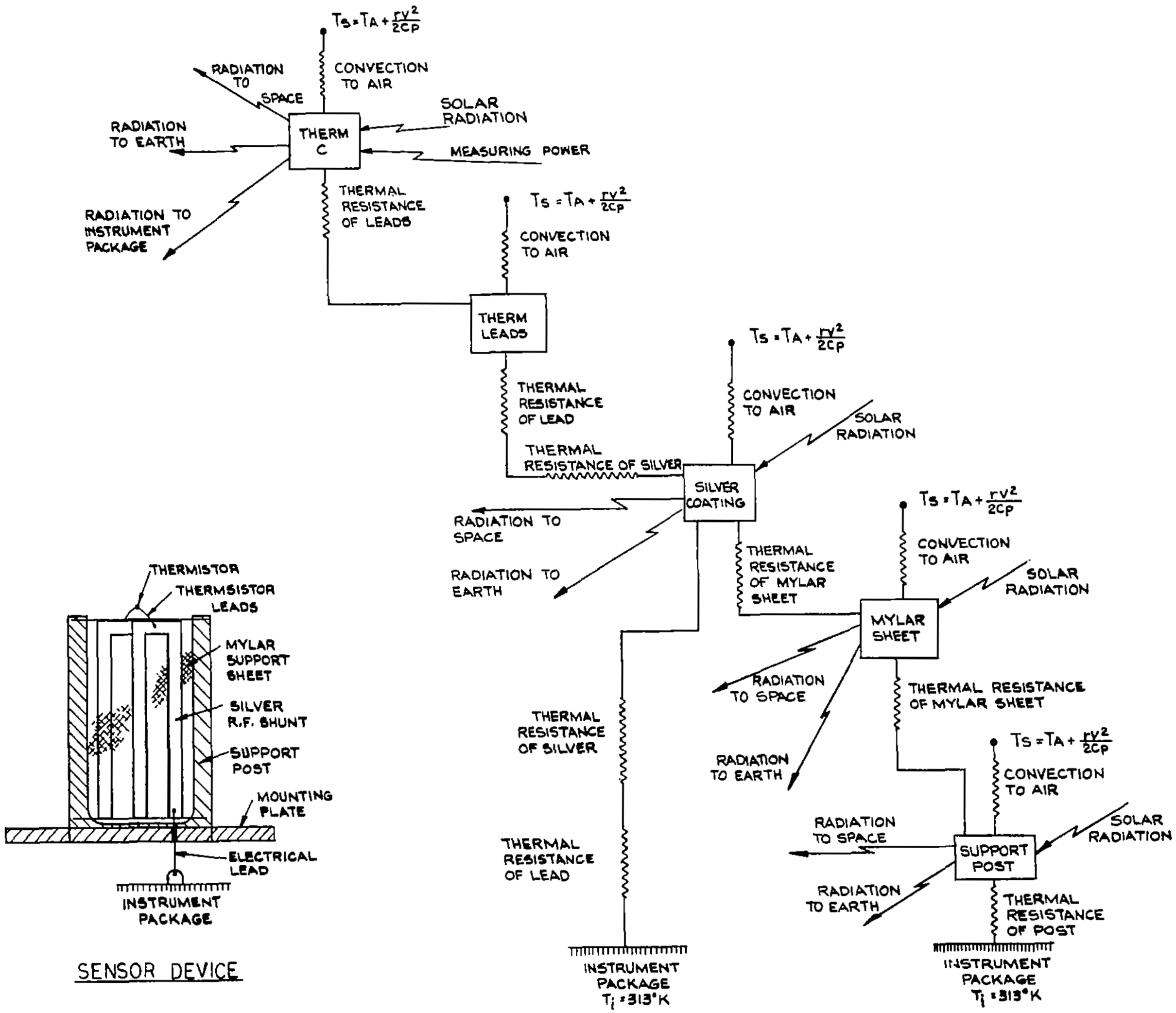

THERMAL MODEL

FIGURE-7

B - Results of Computations

Table 2 gives the summary of the behavior of the thermal model from 70 to 44 kilometers altitude at one kilometer intervals. In this table the following symbols are defined:

Z	Altitude - kilometers
TT	Temperature of thermistor
TL	Temperature of thermistor leads
TM	Temperature of Mylar film
TS	Temperature fo silver film
TP	Temperature of phenolic posts
TR	Recovery temperature
TA	Ambient atmospheric temperature

Note: All temperature data are Kelvin scale.

Table 3 tabulates the departure of the temperatures of all elements of the mount, including the thermistor, from the atmospheric temperature at the various altitudes given. This latter table provides the most valuable insight into the thermal behavior of the sensor and the influence upon it which may be attributed to its physical connection to the instrumentation. For example the following observations may be made from study of this data:

The temperature of the thermistor leads TL as well as the temperature of the deposited silver film TS maintain a close relation to the temperature of the thermistor TT throughout the flight.

The temperature of the Mylar film TM very quickly reaches thermal equilibrium with the recovery temperature TR and, by 56 kilometers, is in equilibrium with the atmospheric temperature. These results imply that the thermistor and the silver film are well isolated from the phenolic support posts whose temperature TP actually increases with descent and remains at a high temperature relative to ambient. Moreover, it may be observed that the Mylar film actually becomes colder than the ambient for a portion of the flight. This is attributed to its poor thermal conductivity, its low absorption coefficient for solar radiation and, its high emissivity.

Of most significance in the data of Tables 2 and 3, however, is the recovery temperature TR and its relation to the thermistor temperature TT. By comparing the difference temperatures of these two parameters at any altitude, the actual error in measurement is obtained. Stated differently: the best measurement that can be obtained from the thermistor is the value of the recovery temperature of the surrounding gas; hence an analysis of the accuracy of the thermistor as a measuring device can only be based upon the difference between its temperature and the temperature of its surrounding environment TR. Table 4 presents the results of such a comparison along with the resulting inaccuracies.

TABLE 2

THERMAL BEHAVIOR OF MODEL
THIN FILM THERMISTOR MOUNT

Z	TT	TL	TS	TM	TP	TR	TA
70	313	313	313	313	313	248.9	219.7
69	295.2	293.1	292.4	295.3	312.9	249.3	223.6
68	281.4	279.8	279.5	282.5	312.7	250.1	227.5
67	272.1	271.0	270.9	273.3	312.6	251.2	231.4
66	266.7	265.9	266.0	267.0	312.4	252.7	235.3
65	264.2	263.6	263.7	262.8	312.2	254.4	239.2
64	263.6	263.1	263.3	260.3	312.1	256.4	243.1
63	264.3	263.9	264.1	259.1	311.9	258.6	247.0
62	265.7	265.3	265.6	258.9	311.7	261.0	250.9
61	267.3	266.9	267.2	259.4	311.5	262.6	253.8
60	267.9	267.4	267.7	260.0	311.3	263.4	255.8
59	268.3	267.9	268.2	260.7	311.1	264.4	257.7
58	268.9	268.5	268.8	261.4	310.9	265.4	259.7
57	269.7	269.3	269.6	262.2	310.7	266.6	261.6
56	270.6	270.2	270.5	263.1	310.4	267.9	263.6
55	271.7	271.3	271.6	264.1	310.2	269.3	265.6
54	272.9	272.5	272.8	265.1	309.9	270.7	267.5
53	274.2	273.8	274.1	266.3	309.7	272.2	269.5
52	275.0	274.6	275.0	267.4	309.4	273.1	270.6
51	274.5	274.1	274.5	267.8	309.1	272.8	270.6
50	274.1	273.7	274.1	267.8	308.8	272.5	270.6
49	273.7	273.3	273.7	267.8	308.3	272.3	270.6
48	273.3	273.0	273.4	267.8	307.8	272.0	270.6
47	272.1	271.7	272.1	267.5	307.2	270.8	269.5
46	269.1	268.6	269.1	265.8	306.3	267.9	266.8
45	266.1	265.7	266.1	263.8	305.0	265.0	264.1
44	263.1	262.7	263.2	261.6	303.4	262.1	261.3

TABLE 3

DIFFERENCE TEMPERATURE VS. ALTITUDE

Z	TT-TA	TL-TA	TS-TA	TM-TA	TP-TA	TR-TA
70	93.3	93.3	93.3	93.3	93.3	29.2
68	53.9	52.3	52.0	55.0	85.2	22.6
66	31.4	30.6	30.7	31.7	77.1	17.4
64	20.5	20.0	20.2	17.2	69.0	13.3
62	14.8	14.4	14.7	8.0	60.8	10.1
60	12.1	11.6	11.9	4.2	55.5	7.6
58	9.2	8.8	9.1	1.7	51.2	5.7
56	7.0	6.6	6.9	-0.5	47.0	4.3
54	5.4	5.0	5.3	-2.4	42.4	3.2
52	4.4	4.0	4.4	-3.2	38.8	2.5
50	3.5	3.1	3.5	-2.8	38.2	1.9
48	2.7	2.4	2.8	-2.8	37.2	1.4
46	2.3	1.8	2.3	-1.0	39.5	1.1
44	1.8	1.4	1.9	0.3	42.1	0.8

TABLE 4

ACCURACY OF TEMPERATURE MEASUREMENT

Z	TT-TA (Deg. K)	TT-TR (Deg. K)	ERROR (% TR)	ERROR (% TA)
70	93.3	64.1	-	-
68	53.9	31.3	12.5	23.7
66	31.5	14.0	5.53	13.4
64	20.5	7.2	2.80	8.44
62	14.8	4.7	1.80	5.9
60	12.1	4.5	1.71	4.74
58	9.2	3.5	1.37	3.55
56	7.0	2.7	1.00	2.66
54	5.3	2.2	0.81	1.98
52	4.4	1.9	0.69	1.63
50	3.4	1.6	0.59	1.26
48	2.7	1.3	0.48	1.0
46	2.3	1.2	0.45	0.86
44	1.8	1.0	0.38	0.69

VI. CONCLUSIONS

Results of error analysis indicate that the contractor's initial objective of achieving essentially complete thermal isolation of the bead thermistor from its mounting and from accompanying instrumentation has been accomplished. This conclusion is based upon the data of Table 2 wherein it is shown that the temperature of the leads is below that of the thermistor throughout the descent.

Hence it appears that only two avenues are open to improve the accuracy of the temperature data: increasing thermistor convection coefficient, and; lowering the ventilation speed. The effect of the latter has been examined by recomputing the thermal model for one-half the initial fall rate. Results are given in Tables 5 and 6. From these data may be seen a significant improvement in accuracy, most of which stems from lower aerodynamic heating. The effect of lowering initial temperature of the thermistor was also examined and was found to have a negligible effect for data below 60 kilometers.

Based upon these analyses and assuming the standard atmospheric profile it is concluded that temperature data as measured by the system described herein is in error by approximately 5 percent at 60 kilometers and does not approach the level of 1 percent until 48 kilometers. If initial altitudes are lower than the starting altitude used herein (70 km) inaccuracies will be even greater than those shown.

TABLE 5

BEHAVIOR OF THERMAL MODEL

ONE-HALF FALL RATE

Z	TT	TL	TS	TM	TR	TA
70	313	313	313	313	227.0	219.7
68	256.7	255.7	255.9	266.2	233.1	227.5
66	249.4	249.0	249.2	252.6	239.6	235.3
64	253.2	252.8	253.1	250.7	246.4	243.1
62	258.7	258.3	258.6	253.1	253.4	250.9
60	262.3	261.9	262.3	256.2	257.7	255.8
58	264.8	264.4	264.8	258.4	261.1	259.7
56	267.6	267.2	267.6	260.7	264.7	263.6
54	270.6	270.2	270.6	263.0	268.3	267.5
52	273.2	272.8	273.3	265.4	271.3	270.6
50	272.7	272.3	272.8	265.8	271.1	270.6
48	272.3	272.0	272.4	266.0	271.0	270.6
46	268.2	267.9	268.4	264.2	267.1	266.8
44	262.5	262.1	262.6	260.6	261.5	261.3

TABLE 6

ACCURACY OF TEMPERATURE MEASUREMENTS

ONE HALF FALL RATE

Z	TT-TA	TT-TR	ERROR % TR	ERROR % TA
70	93.3	86	-	-
68	29.2	23.6	10.1	12.80
66	14.1	9.8	4.1	6.00
64	10.1	6.8	2.76	4.15
62	7.8	5.3	2.09	3.10
60	6.5	4.6	1.79	2.55
58	5.1	3.7	1.42	1.97
56	4.0	2.9	1.1	1.52
54	3.1	2.3	0.86	1.16
52	2.6	1.9	0.70	0.96
50	2.1	1.6	0.59	0.77
48	1.7	1.3	0.48	0.63
46	1.4	1.1	0.41	0.52
44	1.2	1.0	0.38	0.46

REFERENCES

1 - Ney, E.P., Maas R. W., Huch W.F. - Measurement of Atmospheric Temperature, Journal of Meteorology Vol. 18, No. 1, Feb. 1961

2 - Barr, W.C. - Theoretical Considerations in the Design of Atmospheric Temperature Sensing Elements - USASRDL Tech. Report 2195, April 1961 - ASTIA Doc. No. AD 255896

3 - Wagner, N.K. - Theoretical Accuracy of the Meteorological Rocketsonde Thermistor, Elec. Eng'g. Res. Lab., Univ. of Texas, Report No. 7-23, 1963, Contract DA-23-072-ORD-1564

4 - Ballard, H.N. - Response Time of and Effects of Radiation on the VECO Bead Thermistor Tech. Report., Schellinger Res. Lab., Texas Western Coll., April 1961, Contract DA-29-040-ORD-2410

5 - Wright, W.F. - A survey for Naval Ordnance Laboratory of High Altitude Atmospheric Temperature Sensors and Associated Problems, 1961, Contract N-60921-6136

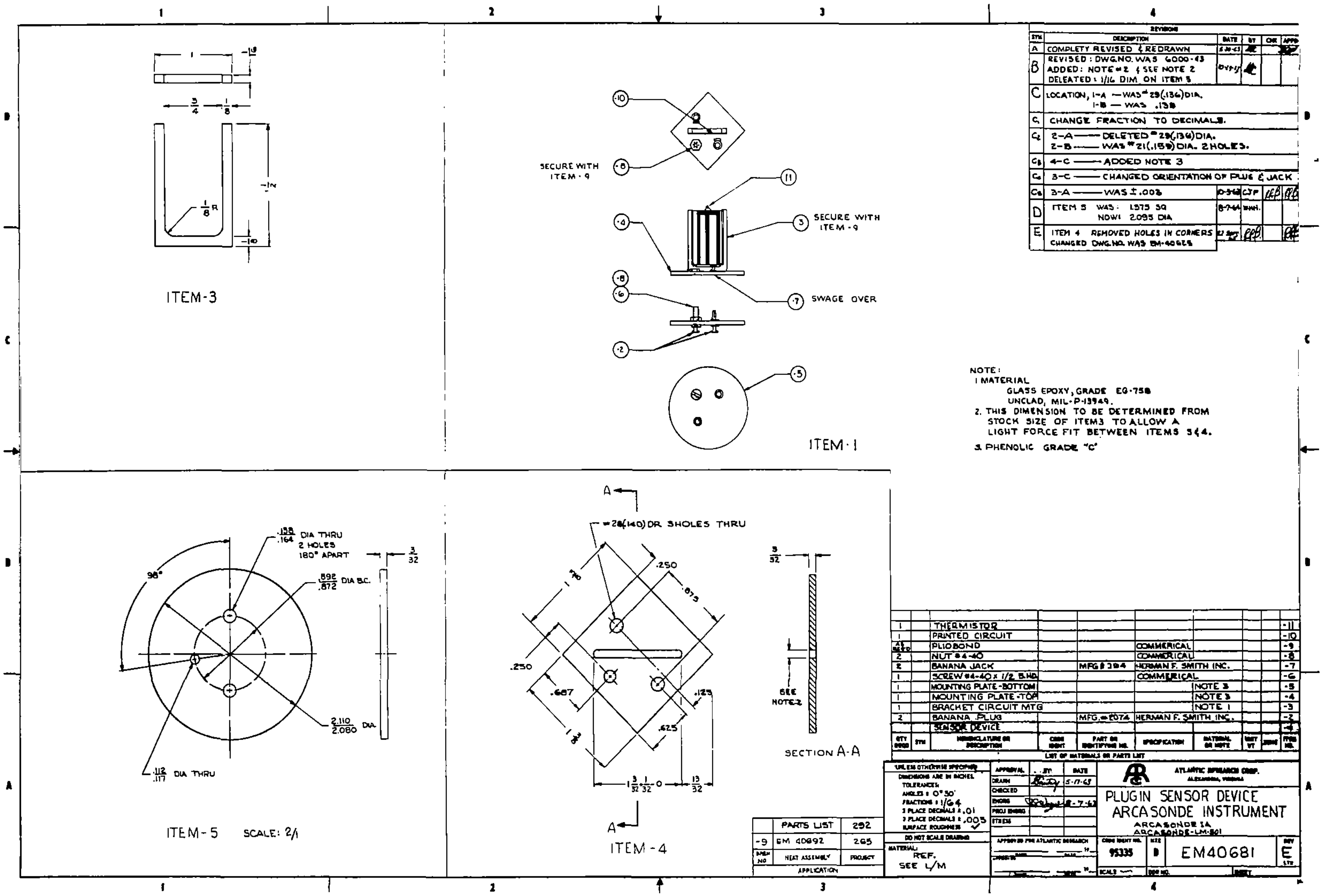

ITEM-3
ITEM·1
ITEM-5 SCALE: 2/1
ITEM-4
SECTION A-A
SECURE WITH ITEM·9
SECURE WITH ITEM·9
SWAGE OVER
.138/.164 DIA THRU 2 HOLES 180° APART
.892/.872 DIA B.C.
2.110/2.080 DIA
.112/.117 DIA THRU
98°
#28(.140) DR. 3 HOLES THRU
.250
.875
.687
.125
.625
SEE NOTE 2
NOTE:
1 MATERIAL
GLASS EPOXY, GRADE EG-758
UNCLAD, MIL-P-13949.
2. THIS DIMENSION TO BE DETERMINED FROM STOCK SIZE OF ITEM3 TO ALLOW A LIGHT FORCE FIT BETWEEN ITEMS 3&4.
3. PHENOLIC GRADE "C"
REVISIONS
A COMPLETY REVISED & REDRAWN
B REVISED: DWG.NO. WAS 6000-43 ADDED: NOTE #2 & SEE NOTE 2 DELEATED: 1/16 DIM ON ITEM 5
C LOCATION, 1-A —WAS #29(.136)DIA. 1-B — WAS .138
C1 CHANGE FRACTION TO DECIMALS.
C2 2-A —— DELETED #29(.136)DIA. 2-B —— WAS #21(.159)DIA. 2HOLES.
C3 4-C —— ADDED NOTE 3
C4 3-C —— CHANGED ORIENTATION OF PLUG & JACK
C5 3-A —— WAS ±.002
D ITEM 5 WAS: 1.575 SQ NOW: 2.095 DIA
E ITEM 4 REMOVED HOLES IN CORNERS CHANGED DWG.NO. WAS EM-40625
1 THERMISTOR -11
1 PRINTED CIRCUIT -10
AS REQ'D PLIOBOND COMMERICAL -9
2 NUT #4-40 COMMERICAL -8
2 BANANA JACK MFG#394 HERMAN F. SMITH INC. -7
1 SCREW #4-40 x 1/2 B.HD. COMMERICAL -6
1 MOUNTING PLATE-BOTTOM NOTE 3 -5
1 MOUNTING PLATE-TOP NOTE 3 -4
1 BRACKET CIRCUIT MTG NOTE 1 -3
2 BANANA PLUG MFG.#2074 HERMAN F. SMITH INC. -2
SENSOR DEVICE -1
LIST OF MATERIALS OR PARTS LIST
PARTS LIST 292
-9 EM 40892 265
NEXT ASSEMBLY PROJECT
APPLICATION
UNLESS OTHERWISE SPECIFIED DIMENSIONS ARE IN INCHES
TOLERANCES: ANGLES ± 0°30' FRACTIONS ± 1/64 2 PLACE DECIMALS ± .01 3 PLACE DECIMALS ± .005
DO NOT SCALE DRAWING
MATERIAL: REF. SEE L/M
DRAWN 5-17-63
ATLANTIC RESEARCH CORP.
PLUGIN SENSOR DEVICE
ARCASONDE INSTRUMENT
ARCASONDE 1A
ARCASONDE-LM-801
95335
D
EM40681
E

APPENDIX

I - ERROR ANALYSIS

A - COMPUTATIONAL PROCEDURE

The thermal model of Figure 1 requires the solution of a system of five first order differential equations with independent and dependent variables. A third order Runge-Kutta method is used. Solution was made on an IBM model 7090 computer. The integration interval was set at 0.002 seconds as a compromise between acceptable accuracy and economy of computer time.

B - EQUATIONS

1 - THERMISTOR

$$\frac{dT_t}{dZ} = \frac{B_{11} \; (T_1 - T_t) - B_{12} \; H_t \; (T_t - T_r) + B_{13} \; (Q_1 - T_t^4) + B_{14}}{V}$$

where

$$B_{11} = \frac{K_1 \; A_{1cr}}{L_1 \; C_t} \qquad B_{12} = \frac{A_{tc}}{C_t}$$

$$B_{13} = \frac{\varepsilon\sigma \; A_{tr}}{C_t} \qquad B_{14} = \frac{a_{ts} \; E_s \; A_{ts} + W}{C_t}$$

2 - THERMISTOR LEADS

$$\frac{dT_1}{dZ} = \frac{-B_{21} \; (T_1 - T_r) - B_{22} \; H_1 \; (T_1 - T_r) - B_{23} \; (T_1 - T_t)}{V}$$

where

$$B_{21} = \frac{K_1 \; K_s \; A_{1cr} \; A_{scr}}{(K_1 \; L_s \; A_{1cr} + K_s \; L_1 \; A_{scr}) \; C_1} \qquad B_{22} = \frac{A_{1c}}{C_1}$$

$$B_{23} = \frac{K_1 \; A_{1cr}}{C_1 \; L_1}$$

3 - PHENOLIC POSTS

$$\frac{dT_p}{dZ} = \frac{B_{31} (T_i - T_p) - B_{32} H_p (T_p - T_r) + B_{33} (Q_2 - T_p^{4})}{V}$$

$$\frac{-B_{34} (T_p - T_m) + B_{35}}{V}$$

where

$$B_{31} = \frac{K_p A_{pcr}}{L_p C_p} \qquad B_{32} = \frac{A_{pc}}{C_p} \qquad B_{33} = \frac{\varepsilon_p \sigma A_{pr}}{C_p}$$

$$B_{34} = \frac{K_m A_{mcr}}{L_m C_p} \qquad B_{35} = \frac{a_{ps} E_s A_{ps}}{C_p}$$

4 - MYLAR FILM

$$\frac{dT_m}{dZ} = \frac{B_{41} (T_p + T_s - 2T_m) - B_{42} H_m (T_m - T_r) + B_{43} (Q_2 - T_m^{4}) + B_{44}}{V}$$

where

$$B_{41} = \frac{K_m A_{mcr}}{L_m C_m} \qquad B_{42} = \frac{A_{mc}}{C_m} \qquad B_{43} = \frac{\varepsilon_m \sigma A_{mr}}{C_m}$$

$$B_{44} = \frac{a_{ms} E_s A_{mr}}{C_m}$$

5 - SILVER FILM

$$\frac{dT_s}{dZ} = \frac{B_{51}\ (T_i - T_s) - B_{52}\ H_s\ (T_s - T_r) + B_{53}\ (Q_2 - T_s{}^4)}{V}$$

$$\frac{+B_{54}\ +B_{55}(T_m-T_s)\ +B_{56}(T_1-T_s)}{V}$$

where

$$B_{51} = \frac{K_1\ K_s\ A_{1cr}\ A_{scr}}{(K_1 L_s A_{1cr} + K_s L_i A_{scr})\ C_s} \qquad B_{52} = \frac{A_{sc}}{C_s} \qquad B_{53} = \frac{\varepsilon_s \sigma\ A_{sc}}{C_s}$$

$$B_{54} = \frac{a_{ss}\ E_s\ A_{sr}}{C_s} \qquad B_{55} = \frac{K_m\ A_{mcr}}{L_m\ C_s} \qquad B_{56} = B_{21}$$

C - MATHEMATICAL SYMBOLS

A_{lc} Area of thermistor leads for convection. (cm^2)

A_{lcr} Cross sectional area thermistor leads. (cm^2)

A_{mc} Area of Mylar for convection. (cm^2)

A_{mr} Area of Mylar for long wave emission. (cm^2)

a_{ms} Absorption coefficient of Mylar for solar radiation.

A_{pc} Area of posts for convection. (cm^2)

A_{pcr} Cross sectional area of posts. (cm^2)

A_{pr} Area of posts for long wave emission. (cm^2)

A_{ps} Effective area of posts for solar radiation. (cm^2)

a_{ps} Absorption coefficient of post for solar radiation

A_{sc} Area of silver for convection. (cm^2)

A_{scr} Cross-sectional area of silver film. (cm^2)

A_{sr} Area of silver for long wave emission. (cm^2)

A_{ss} Effective area of silver for solar radiation. (cm^2)

a_{ss} Absorption coefficient of silver for solar radiation.

A_{tc} Area of thermistor for convection. (cm^2)

A_{tr} Area of thermistor for long wave emission. (cm^2)

a_{ts} Absorption coefficient of thermistor for solar radiation.

A_{ts} Effective area of thermistor to solar radiation. (cm^2)

C_l Heat capacity of leads. ($cal\ K^{-1}$)

C_m Heat capacity of Mylar. ($cal\ K^{-1}$)

C_p Heat capacity of posts. ($cal\ K^{-1}$)

c_p Specific heat of air at constant pressure. ($Km^2\ sec^{-2}\ K^{-1}$)

C_s Heat capacity of silver. ($cal\ K^{-1}$)

C_t Heat capacity of thermistor. ($cal\ K^{-1}$)

E_s Incident solar radiation flux. ($cal\ cm^{-1}\ sec^{-1}$)

H_m Convective heat transfer for Mylar. ($cal\ sec^{-1}$)

H_p	Convective heat transfer of posts. (cal sec^{-1})
H_s	Convective heat transfer for silver. (cal sec^{-1})
H_t	Convective heat transfer for thermistor. (cal sec^{-1})
K_l	Thermal conductivity of thermistor leads. (cal cm^{-1} sec^{-1} K^{-1})
K_m	Thermal conductivity of Mylar. (cal cm^{-1} sec^{-1} K^{-1})
K_p	Thermal conductivity of posts. (cal cm^{-1} sec^{-1} K^{-1})
K_s	Thermal conductivity of silver. (cal cm^{-1} sec^{-1} K^{-1})
L_i	Length of leads to instrument package. (cm)
L_l	Length of thermistor leads. (cm)
L_m	Length of Mylar. (cm)
L_p	Length of posts. (cm)
L_s	Length of silver film. (cm)
Q_1	Effective radiation temperature for thermistor
Q_2	Effective radiation temperature for phenolic posts, Mylar, silver
T_a	Temperature of atmosphere. (deg K)
T_i	Temperature of instrument package. (deg K)
T_l	Temperature of thermistor leads. (deg K)
T_m	Temperature of Mylar. (deg K)
T_p	Temperature of phenolic posts. (deg K)
T_r	Recovery temperature. (deg K)
T_s	Temperature of silver film. (deg K)
T_t	Temperature of thermistor. (deg K)
V	Ventilation speed. (km sec^{-1})
W	Electrical power dissipated by thermistor. (cal sec^{-1})
Z	Geometric altitude. (Kilometers)
σ	Stephan-Boltzmann constant. (cal cm^{-2} sec^{-1} K^{-4})
ε	Emissivity of thermistor for long wave radiation.

ε_s	Emissivity of silver for long wave radiation
ε_p	Emissivity of post for long wave radiation
ε_m	Emissivity of Mylar for long wave radiation

D - SPECIFICATION OF CONSTANTS

1- THERMISTOR

$C_t = 8.03 \times 10^{-6}$

$A_{tc} = 3.217 \times 10^{-3}$

$a_{ts} = 0.072$

$A_{ts} = A_{tr} = 1.608 \times 10^{-3}$

$W = 4.778 \times 10^{-6}$

$E = 0.022$

2- THERMISTOR LEADS

$K_l = 0.166$

$A_{lcr} = 1.013 \times 10^{-5}$

$L_l = 0.16$

$C_l = 2.22 \times 10^{-6}$

$A_{lc} = 5.10 \times 10^{-3}$

3- PHENOLIC POSTS

$K_p = 6.90 \times 10^{-4}$

$A_{pcr} = 0.1088$

$C_p = 0.1653$

$a_{ps} = 0.80$

$A_{pr} = 3.875$

$L_p = 1.905$

$A_{pc} = 6.592$

$\varepsilon_p = 0.80$

$A_{ps} = 1.3564$

4- MYLAR FILM

$K_m = 5.66 \times 10^{-5}$

$A_{mcr} = 1.936 \times 10^{-2}$

$L_m = 0.0761$

$C_m = 1.85 \times 10^{-2}$

$A_{mc} = 14.54$

$A_{mr} = 7.27$

$a_{ms} = 0.06$

$\varepsilon_m = 0.8$

5- SILVER FILM

$K_s = 0.988$

$A_{scr} = 4.064 \times 10^{-4}$

$L_s = 1.70$

$C_s = 7.746 \times 10^{-4}$

$a_{ss} = 0.02$

$A_{sr} = 2.526$

$A_{sc} = 3.305$

ε_s 0.02

6- INSTRUMENT PACKAGE

$T_i = 313$

$L_i = 1.27$

7- GENERAL

$E_s = 0.045$

$\sigma = 1.368 \times 10^{-12}$

II - BASES FOR COMPUTATIONS

A - THE ATMOSPHERE

The environmental temperature distribution used in the computation is that of the 1962 U.S. Standard Atmosphere. Equations used to describe this quantity are those used by others[1] and are given below:

$$T_a = \begin{cases} -3.9016\ Z + 492.775 & 80 \geq Z > 61.5\ \text{km} \\ -1.9584\ Z + 373.268 & 61.5 \geq Z > 52.4\ \text{km} \\ 270.650 & 52.4 \geq Z > 47.4\ \text{km} \\ 2.749\ Z + 140.344 & 47.4 \geq Z > 32.1\ \text{km} \end{cases}$$

B - VENTILATION SPEED

The expression used to specify the ventilation speed (and fall rate) is that used by others[3] which is based upon observational data from White Sands Missile Range for the standard ARCAS sounding rocket system and is as follows:

$$V = 0.000508 \exp(\sqrt{0.81148\ Z - 5.61536} - 1.07395)$$

C - AERODYNAMIC CONSIDERATIONS

1 - Recovery Factor

The method of reference 3 was used to determine aerodynamic heating effect. Equations used to approximate this parameter are:

$$r = \begin{cases} 0.0173\ Z - 0.024 & 80 \geq Z > 53.4\ \text{km} \\ 0.90 & 53.4 \geq Z > 30.0\ \text{km} \end{cases}$$

2 - Flow Regime

The thermistor is considered in slip flow for Knudsen numbers greater than 0.10. Transition to continuum flow thus occurred at approximately 42 kilometers. Thermistor convection coefficients were computed from the general expression[2]:

1 See text reference 3, Wagner, N.K.

$$H_t = \frac{K \; Nu^o}{D}$$

where H_t = Convection coefficient
K = Thermal conductivity of air
D = Diameter of thermistor
Nu^o = Nusselt number for continuum flow

Corrections to Nu^o for slip flow were made according to the expression:

$$Nu = \frac{Nu^o}{1 + 3.42 \frac{M}{R_e P_r} Nu^o}$$

where Nu = Nusselt number for slip flow
M = Mach number
R_e = Reynolds number
P_r = Prandtl number

3 - Leads

Nusselt numbers for continuum flow were determined from the expression for a cylinder:

$$N = C \; (R_e)^m$$

where $C, m = f\;(R_e)$

For slip flow, corrections were made in accordance with the method used for the thermistor.

4 - Mylar, Silver, Phenolic Post

Nusselt numbers were determined for flat plates in accordance with procedures of Eckart[1]. To determine average heat transfer over the total areas, the computed values of Nu were doubled. These parts of the mount remain in continuum flow throughout descent.

1 Eckart, E.R.G. - Introduction to the Transfer of Heat and Mass, McGraw Hill Book Co., 1950.

D - RADIATION EFFECTS

Incident solar radiation flux is considered a constant for all parts of the mount except the thermistor leads. Because of the very small area, radiation effect on the latter was omitted. For the purpose of computing the loss of heat by emission from the parts various emissivity values were assumed for the several parts. The effective radiation temperatures of concern are expressed by the following:

$$Q_1 = 0.5T_e^4 + 0.06T_i^4 + 0.44T_{as}^4$$

$$Q_2 = 0.5T_e^4 + 0.5T_{as}^4$$

where T_e is the blackbody radiation temperature below the thermistor; T_i is the instrument temperature (313 deg K), and; T_a is the blackbody radiation temperature of the atmospheric environment above the thermistor. T_e and T_{as} are estimated from a solution of the following expressions:

$$T_e = 249.6 - 0.09 Z$$

$$T_{as} = 123.3 - 1.25 Z$$

E - ELECTRICAL POWER DISSIPATION

The power dissipation in the thermistor is considered to stem from two sources: the direct current used to electrically measure the resistance of the bead and, the radiofrequency energy absorbed by the thermistor circuit which emanates from the telemetering transmitter. The former is a function of the thermistor temperature and its external measuring circuit. Laboratory tests of the Arcasonde 1A instrument show that measuring current power dissipated in the thermistor does not exceed 4.5 microwatts at any temperature. Radiofrequency power absorbed by the thermistor has been measured indirectly in the laboratory by observing and measuring the change in the pulse repetition rate of the measuring circuit when the telemetering transmitter is energized and deenergized. This change, when converted to a change in temperature of the bead, shows an average increase in bead temperature of about 0.1° Centrigrade. Based upon the Victory Engineering Co. published dissipation constant of 0.01°C/microwatt at earth's surface, it is estimated that 10-15 microwatts of RF power is normally absorbed by the bead.

For the purpose of the computations reported herein a constant power dissipation of 20 microwatts was assumed.